Corrosion inhibition of mild steel by benzotriazole derivatives in acidic medium

S. TAMIL SELVI, V. RAMAN and N. RAJENDRAN*
Department of Chemistry, Anna University, Chennai 600 025, India
*(*author for correspondence, e-mail: nrajendran@annauniv.edu)*

Abstract

Benzotriazole derivatives, namely, *N*-[1-(benzotriazolo-1-yl)alkyl] aryl amine (BTMA), *N*-[1-(benzotriazolo-1-yl)aryl] aryl amine (BTBA), and 1-hydroxy methyl benzotriazole (HBTA), were synthesized and their inhibition behaviour on mild steel in 0.5 M H_2SO_4 at room temperature was investigated by various techniques. Preliminary screening of the inhibition efficiency (IE) was carried out using weight-loss measurements. Potentiodynamic polarization and AC impedance studies were used to investigate the inhibitor mechanism. Benzotriazole derivatives were found to act as mixed type inhibitors. Among the compounds studied, HBTA exhibited the best performance giving more than 95% IE in H_2SO_4 solutions. The passive film characterization was done using FTIR spectrum.

1. Introduction

Mild steel has been extensively used under different conditions in chemical and allied industries in handling alkaline, acid and salt solutions. Chloride, sulphate and nitrate ions in aqueous media are particularly aggressive and accelerate corrosion. One way of protecting mild steel from corrosion is to use corrosion inhibitors. Most of the well-known inhibitors are organic compounds containing nitrogen, sulphur and/or oxygen atoms. It has been observed that most of the organic inhibitors act by adsorption on the metal surface [1]. This phenomenon is influenced by the nature and surface charge of metal, by the type of aggressive electrolyte and by the chemical structure of inhibitors.

The adsorption of corrosion inhibitor depends mainly on physico-chemical properties of the molecule such as functional groups, steric factor, molecular size, molecular weight, molecular structure, aromaticity, electron density at the donor atoms and π-orbital character of donating electrons [2–6] and also on the electronic structure of the molecules [7, 8]. Many studies have been made on the corrosion and inhibition of steels in acid media [9–13]. It is well-known that triazole type organic compounds are good inhibitors for many metals and alloys in various aggressive media [14–19].

In the present work, the electrochemical behaviour of mild steel in 0.5 M H_2SO_4 in the absence and presence of benzotriazole derivatives has been investigated by potentiodynamic polarization, electrochemical impedance and weight-loss measurements.
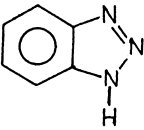
2. Experimental data

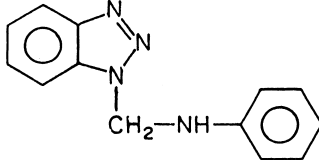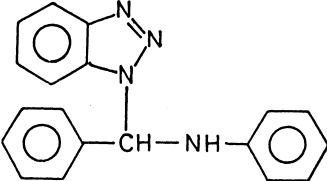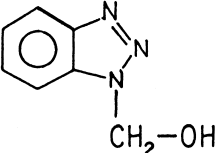### 2.1. *Weight-loss studies*

Mild steel strips having chemical compositions 0.14% C, 0.17% Si, 0.35% Mn, 0.03% P, 0.025% S, the remainder being Fe, were used. Weight-loss measurements were carried out using steel strips of size 8 cm × 5 cm × .4 cm. *N*-(1-benzotriazole-1-yl)methyl] aniline (BTMA) and *N*-(1-benzotriazole-1-yl)benzyl] aniline (BTBA) and 1-hydroxy methyl benzotriazole (HBTA) were synthesized according to a previously reported experimental procedure [20]. The compounds synthesized were characterized by their infrared (IR) spectral data. The molecular structure of BTA, BTMA, BTBA and HBTA are given in the Table 1. The acidic solution used were made using analytical grade H_2SO_4. The concentration range of inhibitors was varied from 0.415 M × 10^{-4} to 3.32 M × 10^{-4} in 0.5 M H_2SO_4.

The weight-loss measurements were carried out as described elsewhere [21]. Mild steel strips were immersed in 400 cm^3 of inhibited and uninhibited solutions at room temperature (25 °C), according to ASTM standards for 2 h in 0.5 M H_2SO_4 solution [22]. The inhibition efficiency (IE) and corrosion rates in the presence of the inhibitors were calculated from weight-loss measurements.

2.2. *Potentiodynamic polarization studies*

The potentiodynamic polarization studies were carried out with steel strips having an exposed area of 1 cm^2.

Table 1. Name and molecular structures of the benzotriazole derivatives

S. no	Designation	Structural formula	Abbreviation
1	Benzotriazole		BTA
2	*N*-[1-(benzotriazolo-l-yl)methyl] aniline		BTMP
3	*N*-[1-(benzotriazolo-l-yl)benzyl] aniline		BTBA
4	1-hydroxy methyl benzotriazole		HBTA

The specimens were mechanically polished using different grades of emery paper (120, 400, 800,1000 and 1200) and washed thoroughly with distilled water and degreased with acetone. The cell assembly consisted of mild steel as working electrode, a platinum foil as counter electrode, and a saturated calomel electrode (SCE) as a reference electrode with a Luggin capillary bridge. Potentiodynamic polarization studies were carried out using a potentiostat/galvanostat (model PGSTAT 12) and the obtained data were analysed using the GPES software version 4.9. At a constant scan rate of 1 mV s^{-1} from open-circuit potential (OCP), anodic and cathodic polarization curves were obtained after immersion of the electrode in the aerated solution for 30 min until reaching steady state. The inhibitor efficiencies of the compounds were determined from corrosion currents calculated using the Tafel extrapolation method.

2.3. *Electrochemical A.C. impedance studies*

Electrochemical impedance spectra (EIS) were carried out at E_{corr} using an electrochemical system Frequency Response Analyser (FRA), which included a potentiostat model PGSTAT 12. Mild steel with the exposed surface of 1 cm^2 was used as the working electrode. The EIS were acquired in the frequency range 100 kHz to 1 Hz with a 10 mV amplitude sine wave generated by a frequency response analyzer.

2.4. *Fourier transform infrared (FTIR) spectroscopic studies*

The mild steel specimens were immersed in various test solutions for a period of 24 h. After 24 h, the specimens were taken out and dried. The surface film was scratched carefully and the product obtained was thoroughly mixed so as to make it uniform throughout. FTIR spectra were recorded using a Perkin–Elmer spectrophotometer Avatar Model from the KBr wafer of the corrosion product.

3. Results and discussion

3.1. *Weight-loss studies*

Table 2 shows the IE and corrosion rate of mild steel obtained by weight-loss measurements at different inhibitor concentrations in 0.5 M H$_2$SO$_4$ at room temperature. The IE was calculated as follows:

$$\text{Inhibition efficiency (IE \%)} = \frac{W - W_{\text{inh}}}{W} \times 100$$

where W_{inh} and W are the values of the weight-loss of steel after immersion in solutions with and without inhibitor, respectively. Table 2 and Figure 1 shows that the IE increases and the corrosion rate decreases with

Table 2. IE for various concentration of benzotriazole derivatives for the corrosion of mild steel in 0.5 M H_2SO_4 obtained from weight-loss measurements at 30 °C

Concentration /M × 10^{-4}	Corrosion rate /mm year^{-1}	Inhibition efficiency /%
0.5 M H_2SO_4	40.83	–
BTA		
4.19	30.82	24.52
8.39	21.57	47.17
16.78	16.12	60.51
25.18	14.64	64.14
33.57	10.79	73.57
41.97	11.55	71.71
BTMA		
2.22	29.27	28.31
4.44	16.18	60.37
8.88	12.23	70.04
13.32	7.70	81.14
17.76	8.48	79.23
BTBA		
1.65	13.87	66.03
3.30	11.94	70.75
6.61	5.39	86.80
9.92	1.54	96.22
13.23	1.70	95.84
HBTA		
3.35	13.48	66.99
6.70	3.85	90.57
13.41	0.616	98.49
20.11	0.385	99.05
26.82	0.693	98.30

increase in inhibitor concentration. The percentage IE for different triazole derivatives decreases in the following order:

HBTA > BTBA > BTMA > BTA

3.1.1. *Mechanism of corrosion inhibition*

It is well-known that the inhibitive action of organic compounds containing S, N and/or O is due to the formation of a co-ordinate type bond between the metal and the lone pair of electrons in the additive. The tendency to form a co-ordinate bond and hence the extent of inhibition can be enhanced by increasing the effective electron density at the functional group of the additive [23]. In aromatic or heterocyclic ring compounds the effective electron density at the functional group can be varied by introducing different substituents in the ring leading to variations of the molecular structure.

The adsorption of benzotriazole derivatives on the metal surface can occur either directly on the basis of donor–acceptor interactions between the π-electrons of the inhibitor and the vacant d-orbitals of iron surface atoms or an interaction of inhibitor with already adsorbed sulphate ions as proposed earlier [24, 25]. The corrosion inhibition property of the BTA derivatives can be attributed to the presence of heteroatoms such as N, O and of π-electrons on aromatic nuclei. These factors play the vital role in the adsorption of the inhibitor on the metal surface.

The corrosion inhibition study indicated that HBTA has the highest IE compared to other BTA derivatives. The high solubility of HBTA in 0.5 M H_2SO_4 and the presence of an oxygen atom with a lone pair of electrons make HBTA a very good inhibitor. Though BTBA and BTMA have an extra phenyl ring, this ring strongly reduces their solubility and they are sterically hindered from adhering to the metal surface through the nitrogen atom. Comparing BTBA and BTMA, BTBA performs better. This is probably due to the influence of the second phenyl ring in the structure. Though the second ring might reduce the solubility further, the π-electron delocalization is greater than the solubility factor.
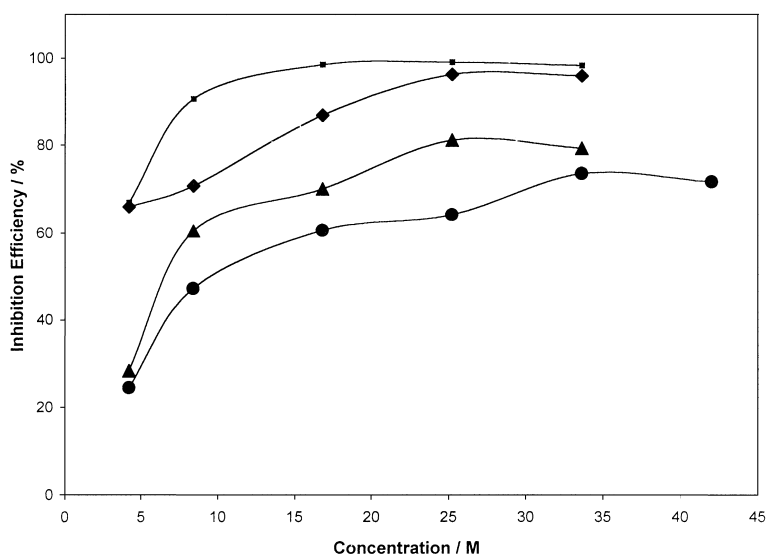

Fig. 1. Variation of IE with inhibitor concentration (M) in 0.5 M H_2SO_4. –●– BTA, –▲– BTMA, –◆– BTBA and –■– HBTA.

3.2. *Potentiodynamic polarization studies*

The cathodic and anodic polarization curves of mild steel in 0.5 M H_2SO_4 solution with maximum concentrations of BTA, BTMA, BTBA and HBTA are shown in Figures 2–6. In the presence of inhibitor, the cathodic and anodic curves are shifted and the shift is dependent on inhibitor concentration.
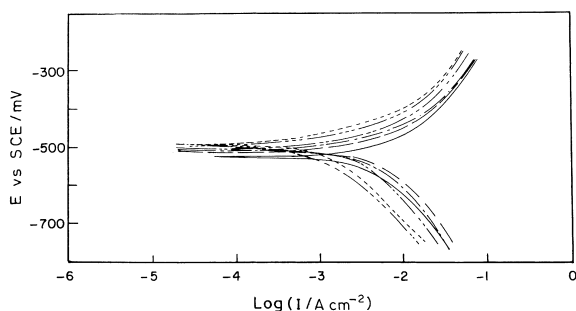

Fig. 2. Polarization curves for mild steel in 0.5 M H_2SO_4 containing different concentrations benzotriazole (BTA). — Blank, — — 8.39 M × 10^{-4}, – · – · – 16.78 M × 10^{-4}, — · · · — 25.18 M × 10^{-4}, – · · · – 33.57 M × 10^{-4} and – – – – 41.97 M × 10^{-4}.
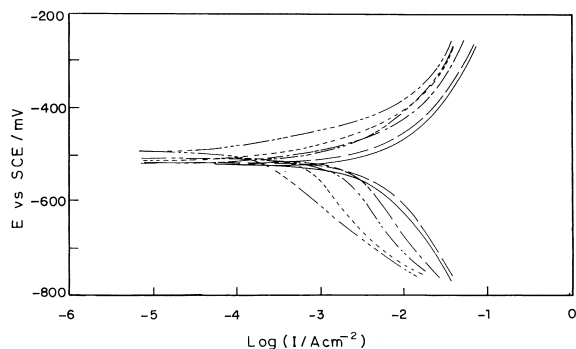

Fig. 3. Polarization curves for mild steel in 0.5 M H_2SO_4 containing different concentrations of *N*-[1-(benzotriazolo-1-yl)methyl]aniline (BTMA). — Blank, — — 2.22 M × 10^{-4}, – · · · · – 4.44 M × 10^{-4}, – · · – 8.88 M × 10^{-4}, – · · · · – 13.32 M × 10^{-4} and – – – – 17.76 M × 10^{-4}.
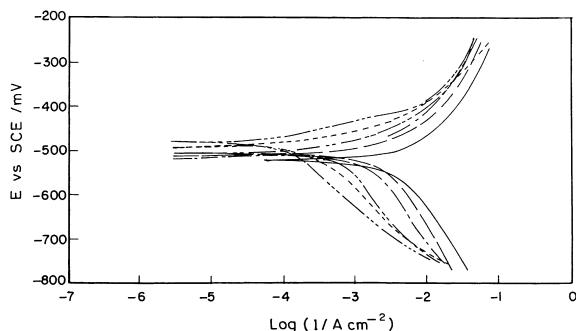

Fig. 4. Polarization curves for mild steel in 0.5 M H_2SO_4 containing different concentrations of *N*-[1-(benzotriazolo-1-yl)benzyl]aniline (BTBA). — Blank, — — 1.65 M × 10^{-4}, – · · · · – 3.30 M × 10^{-4}, – · · · – 6.61 M × 10^{-4}, – · · · · – 9.92 M × 10^{-4} and – – – – 13.23 M × 10^{-4}.
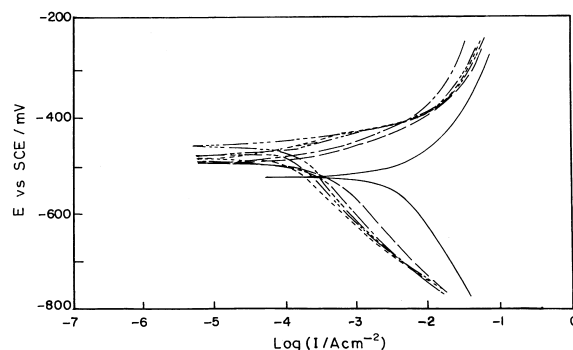

Fig. 5. Polarization curves for mild steel in 0.5 M H_2SO_4 containing different concentrations of 1-hydroxy methyl benzotriazole (HBTA). — Blank, — — 3.35 M × 10^{-4}, – · · · · – 6.70 M × 10^{-4}, – · · · – 13.41 M × 10^{-4}, – · · · · – 20.11 M × 10^{-4} and – – – – 26.82 M × 10^{-4}.
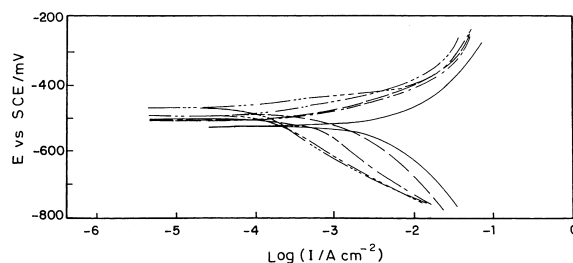

Fig. 6. Cathodic and anodic polarization curves for mild steel in 0.5 M H_2SO_4 containing maximum concentration of benzotriazole derivatives. — Blank, — — BTA, – · · · · – BTMA, – · · · – BTBA and — · · · — HBTA.

The polarization parameters such as corrosion potential (E_{corr}) and corrosion current density (I_{corr}) obtained by extrapolation of the Tafel lines are listed in Table 3. As the concentration of inhibitor increases, there is a marginal shift in E_{corr} and a decrease in I_{corr}. The addition of benzotriazole derivatives hinders acid attack on the mild steel and a comparison of curves in both cases, shows that, with respect to the blank, increasing the inhibitor concentration gives rise to a consistent decrease in anodic and cathodic current densities, indicating that the benzotriazole derivatives act as mixed type inhibitors.

The values of cathodic Tafel slope b_c for benzotriazole derivatives are found to change with inhibitor concentration, which clearly indicates that the benzotriazole derivatives influence the kinetics of the hydrogen evolution reaction. However, the values of the anodic Tafel slope b_a, increases only to a small extent, as these compounds do not influence anodic dissolution. This indicates an increase in the energy barrier for proton discharge, leading to less gas evolution. The values of IE increase with increase in inhibitor concentration, indicating that a higher surface coverage was obtained in a solution with maximum concentration of inhibitor. The corrosion rate in blank solution was found to be 36.38 mm year^{-1} and it was minimized by adding the inhibitors to a lower value of 6.05, 7.60, 1.74 and 0.96 mm year^{-1} for mild steel.

Table 3. Electrochemical parameters and inhibition efficiency for corrosion of mild steel in 0.5 M H_2SO_4 containing different concentrations of benzotriazole derivatives

Concentration /M $\times 10^{-4}$	I_{corr} /μA cm^{-2}	E_{corr} /mV vs. SCE	b_a, /mV (dec)$^{-1}$	b_c, /mV (dec)$^{-1}$	Corrosion rate /mm year^{-1}	Inhibition efficiency /%
Blank	2882	−524	182	117	36.38	−
BTA						
4.19	2296	−510	112	60	29.17	20.33
8.39	1583	−507	128	75	20.48	45.07
16.78	1196	−502	132	82	15.48	58.50
25.18	1085	−498	175	96	14.04	62.35
33.57	837	−496	166	78	6.059	70.95
41.97	842	−497	171	75	6.105	70.78
BTMA						
2.22	2088	−517	123	86	27.02	27.55
4.44	1218	−502	158	87	15.76	57.73
8.88	898	−511	182	90	13.42	68.84
13.32	588	−506	233	74	7.608	79.59
17.76	600	−506	121	53	7.774	79.18
BTBA						
1.65	1060	−497	153	64	13.72	63.21
3.30	895	−495	163	62	11.59	68.94
6.61	404	−498	155	71	5.23	85.98
9.92	134	−493	137	49	1.74	95.35
13.23	141	−493	141	50	1.83	95.10
HBTA						
3.35	982	−499	148	65	12.04	65.92
6.70	308	−496	158	59	2.80	89.31
13.41	86	−481	142	39	1.10	97.05
20.11	74	−469	143	42	0.96	97.43
26.82	81	−478	97	24	1.00	97.18

3.3. *A.C. impedance studies*

The results can be interpreted in terms of the equivalent circuit of the double layer shown in Figure 7, which has been used previously to model the iron-acid interface [26].

The corrosion behaviour of mild steel in acid solution in the presence of benzotriazole derivatives was investigated by EIS at room temperature. Various impedance parameters such as charge transfer resistance (R_{ct}), double layer capacitance (C_{dl}), corrosion current density (I_{corr}) and IE are given in Table 4. The impedance diagrams obtained were not perfect semicircles. This feature had been attributed to frequency dispersion [27]. The charge transfer resistance values (R_{ct}) were calculated from the difference in impedance at the lower and higher frequencies, as suggested by Haruyama and Tsuru [28]. To obtain the double layer capacitance (C_{dl}), the frequency at which the imaginary component
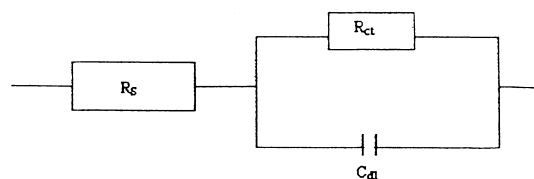
of the impedance is maximum ($-Z''_{max}$) was found and C_{dl} values were obtained from the equation:

$$C_{dl} = \frac{1}{2\pi f(-Z_{im\,max})R_t}$$

Nyquist plots of mild steel in inhibited and uninhibited acidic solutions containing maximum concentrations of benzotriazole derivatives are shown in Figures 8–10. The percentage inhibition efficiency (IE %) for the corrosion of steel is calculated by R_{ct} as follows:

$$\text{Inhibition Efficiency (IE \%)} = \frac{R_{ct}^{-1} - R_{ct\,inh}^{-1}}{R_{ct}^{-1}} \times 100$$

where R_{ct} and $R_{ct\,inh}$ are the charge transfer resistance values without and with inhibitor, respectively. After 20 h immersion, IE increases with increase in inhibitor concentration in 0.5 M H_2SO_4 solution. The IE values determined using the polarization curves were lower than those determined by EIS experiments. This difference is probably due to the shorter immersion time in the case of the polarization measurements [29].

Impedance parameters derived from these investigations are given in Table 4. As the benzotriazole concentration increased, R_{ct} values increased, but C_{dl} values tended to decrease. The decrease in C_{dl} values was

Fig. 7. Equivalent circuit for the metal-acid interface.

Table 4. Impedance measurements and inhibition efficiency in 0.5 M H_2SO_4 containing maximum concentrations of benzotriazole derivatives after immediate immersion, 10 and 20 h immersion

Inhibitors	R_{ct} /ohm cm^2			$E_{rest\ potential}$ vs. SCE /mV			C_{dl} /μF cm^{-2}			Inhibition efficiency /%		
	0 h	10 h	20 h	0 h	10 h	20 h	0 h	10 h	20 h	0 h	10 h	20 h
Blank	6.73	7.00	7.35	−520	−517	−517	1503.2	1365.0	1317.1	−	−	−
BTA	16.91	26.16	29.58	−510	−500	−498	1140.1	128.4	118.3	60.21	73.25	75.16
BTMA	28.31	36.17	39.36	−500	−490	−486	130.5	115.2	105.6	76.23	80.65	81.33
BTBA	40.78	123.23	223.40	−490	−463	−458	117.9	108.2	100.0	83.50	94.32	96.71
HBTA	61.85	258.30	2534.4	−465	−460	−455	95.6	89.3	85.9	89.12	97.29	99.71

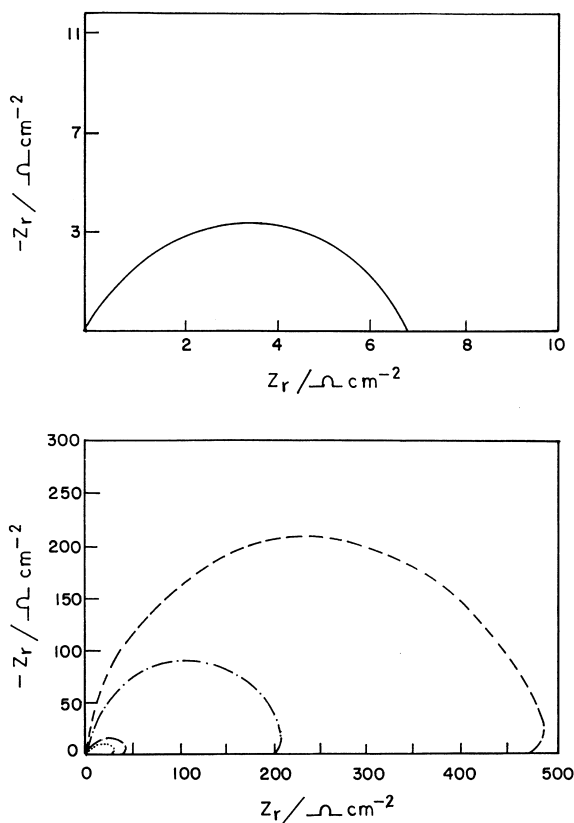*Fig. 8.* Nyquist diagrams for mild steel in 0.5 M H_2SO_4 containing maximum concentration of benzotriazole derivatives after 20 h. — Blank, ... BTA, — — BTMA, – – – – BTBA and – – – – HBTA.
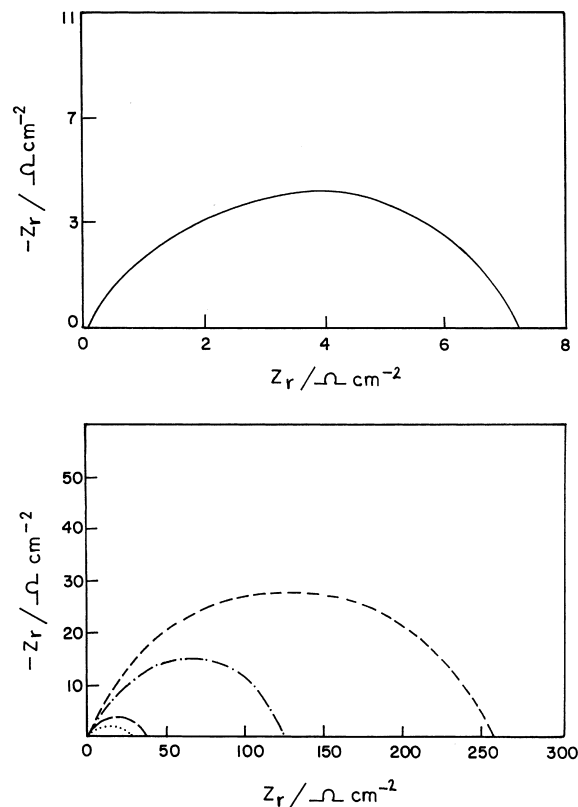

Fig. 9. Nyquist diagrams for mild steel in 0.5 M H_2SO_4 containing maximum concentration of benzotriazole derivatives after 10 h. — Blank, ... BTA, — — BTMA, – – – – BTBA and – – – – HBTA.
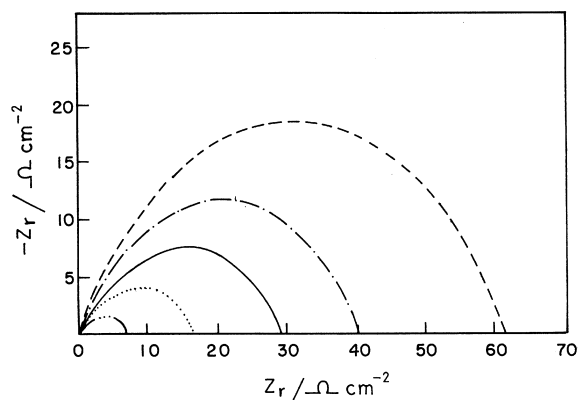

Fig. 10. Nyquist diagram for mild steel in 0.5 M H_2SO_4 containing maximum concentration of benzotriazole derivatives immediately after immersion. — - - – Blank, ... BTA, —— BTMA, – - - – – BTBA and – – – – HBTA.

caused by adsorption of benzotriazole. The relationship between R_{ct} and C_{dl} values with immersion time of 20, 10 h and after immersion are shown in Table 4. R_{ct} values for mild steel in 0.5 M H_2SO_4 without inhibitor (Blank) increased with immersion time, but R_{ct} values for mild steel in 0.5 M H_2SO_4 with optimum concentrations of all the BTA derivatives increased with decrease in immersion time.

When the inhibitor concentration increased, C_{dl} decreased. Decrease in C_{dl}, which can result from a decrease in local dielectric constant and/or an increase in the thickness of the electrical double layer, suggests that the benzotriazole derivatives function by adsorption at the metal-solution interface [30]. The relationship between C_{dl} with immersion time for mild steel in H_2SO_4 without inhibitor (blank) decreased with immersion time
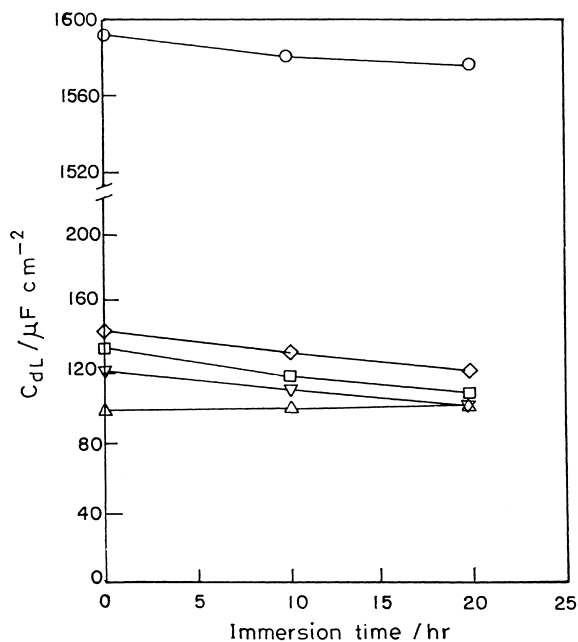
Fig. 11. Relationship between C_{dl} and immersion time for mild steel in –O– Blank, –◇– BTA, –□– BTMA, –▽– BTBA and –△– HBTA.

as shown in Figure 11. The same trend was observed for H_2SO_4 with inhibitor. The change in R_{ct} and C_{dl} values was caused by the gradual replacement of water molecules by the anions of the acid and adsorption of the organic molecules on the metal surface, reducing the extent of dissolution [31].

3.4. *Analysis of FTIR spectra*

The FTIR analysis of BTA, BTBA, BTMA and HBTA and their iron complexes was carried out between 500 and 4000 cm^{-1}. The spectra are shown in Figure 12. The N—H stretching of the BTA derivatives showed a sharp intense peak around 3450 cm^{-1}. The aliphatic and aromatic C—H stretching produced a less intense peak between 2900 and 3100 cm^{-1}. The N—H bends are shown around 1500–1600 cm^{-1} and the C—N stretching vibrations are shown with an intense peak around 1300–1450 cm^{-1}.

The IR spectrum of BTA and BTA-iron complex is shown in Figure 12(a). The broad envelope between 3000 and 3700 cm^{-1} is assigned to the O—H stretch of water. The broadening of the O—H stretch clearly demonstrates the formation of an ice of water over iron oxide, through hydrogen bonding interaction. The presence of the N—H stretch of BTA is not resolved in this region for the BTA-iron complex. However, the presence of BTA over the oxide surface is well evidenced by the aromatic C—H stretch lying just above 3000 cm^{-1}. The peak around 1650 cm^{-1} is assigned to OH_2 bending vibration. The peak around 1000 cm^{-1} in the BTA-iron complex is due to O—Fe—O vibration.

Figure 12(b) illustrates the middle infrared spectrum of BTBA and the BTBA-iron complex. The FTIR spectrum of BTBA-iron complex illustrates a much-broadened envelope for the O—H stretching mode of water. The peaks around 3000 cm^{-1} are due to the aromatic and aliphatic C—H stretching modes. These
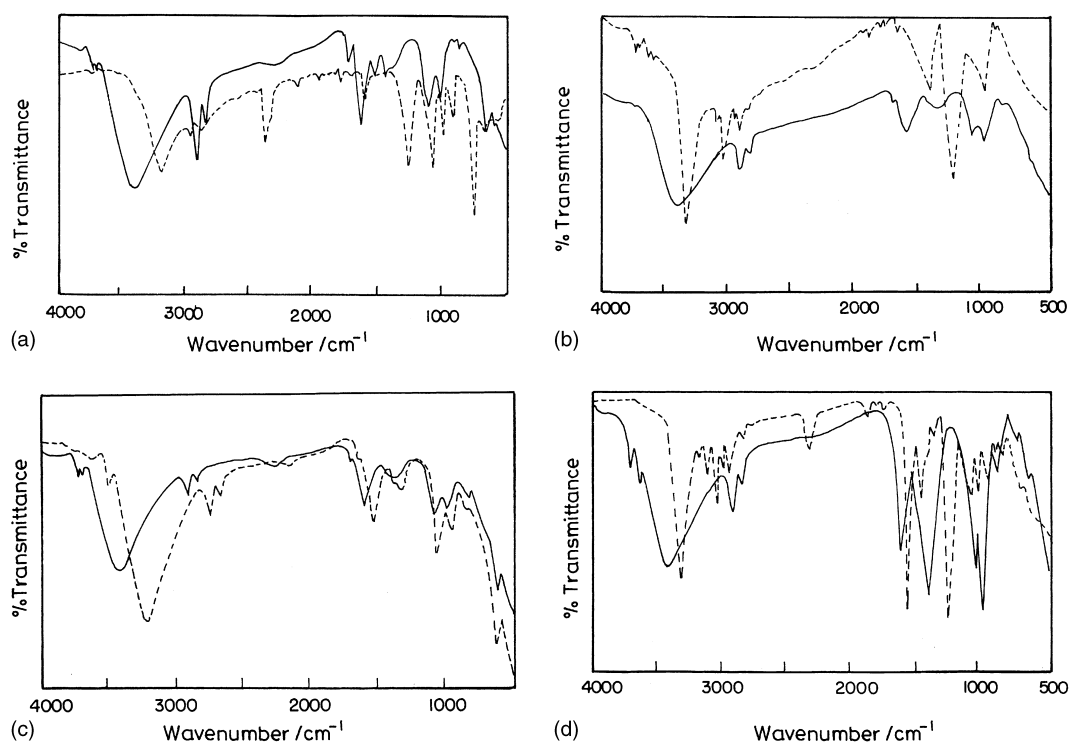

Fig. 12. FTIR spectra (a) – – – – BTA, —— BTA-iron complex (b) – – – – BTMA, —— BTMA-iron complex (c) – – – – BTBA, —— BTBA-iron complex (d) – – – – HBTA, —— HBTA-iron complex.

modes are evidence for the presence of BTBA over the iron oxide.

Figure 12(c) shows the IR-spectrum of BTMA and BTMA-iron complex. The appearance of a shoulder in this envelope at 3300 cm^{-1} due to asymmetric and symmetric stretching modes of CH$_2$ clearly established the presence of the derivative on the iron oxide surface. The sharp peak at 1632 cm^{-1} is assigned to the OH$_2$ bending mode. Below 1500 cm^{-1} the characteristic iron oxide vibrations are evident.

Figure 12(d) illustrates the FTIR spectrum of HBTA and HBTA-iron complex. The broad envelope in the higher energy side can be assigned to ─OH stretch of water. The peak at 1632 cm^{-1} is due to ─OH$_2$ bend. The peak at above 3000 cm^{-1} clearly establishes the presence of HBTA over iron oxide. Although the ─OH stretch (3300 cm^{-1}) is not well resolved, the presence of a shoulder is evident in the broad envelope. The iron oxide vibrations at 1450 cm^{-1} and just above 1000 cm^{-1} are clearly observed. From the foregoing the presence of benzotriazole derivatives on iron oxide surface, is evident.

4. Conclusion

The main conclusions are:
(1) All the substituted benzotriazole derivatives show good IE in 0.5 M H$_2$SO$_4$.
(2) The IE of the substituted benzotriazole derivatives follows the order:
 HBTA > BTBA > BTMA > BTA.
(3) The polarization data indicate suppression of both the partial corrosion processes in the presence of benzotriazole derivatives. These inhibitors behave as mixed-type.
(4) The inhibition is due to the adsorption of benzotriazole derivatives on the steel surface and the blocking of active sites.
(5) Electrochemical impedance spectroscopy shows that R_{ct} values increase, while C_{dl} and I_{corr} values decrease in the presence of benzotriazole derivatives.
(6) FTIR shows that the protective film consists of BTA derivatives.

Acknowledgement

References

1. S.S. Abd EL-Rehim, M.A.M. Ibrahim and K.F. Khaled, *J. Appl. Electrochem.* **29** (1999) 593.
2. E. Khamis, *Corrosion* **46** (1990) 476.
3. E. Stupnisek-Lisac and S. Podbrscek, *J. Appl. Electrochem.* **24** (1994) 779.
4. G. Schmitt and K. Bedbur, *Werkst. Korros.* **36** (1985) 273.
5. I.L. Rosenfeld, 'Corrosion Inhibitors' (McGraw-Hill, New York, 1981).
6. E. Stupnisek-Lisac and M. Metikos-Hukovic, *Brit. Corros. J.* **28** (1993) 74.
7. S.L. Granese, B.M. Rosales, C. Oviedo and J.O. Zerbino, *Corros. Sci.* **33** (1992) 1439.
8. S.L. Granese, *Corrosion* **44** (1988) 322.
9. B. Sathianandhan, K. Balakrishnan and N. Subramanyan, *Br. Corros. J.* **5** (1970) 270.
10. F. Zucchi, G. Trabanelli and G. Brunoro, *Corros. Sci.* **33** (1992) 1135.
11. J. O'M. Bockris and B. Yang, *J. Electrochem. Soc.* **138** (1991) 2237.
12. G. Banerjee and S.N. Malhotra, *Corrosion* **48** (1992) 10.
13. J. Uhrea and G. Aramaki, *J. Electrochem. Soc.* **138** (1991) 3245.
14. A.B. Tadros and B.A. Abdenaby, *J. Electroanal. Chem.* **246** (1988) 433.
15. R.J. Chin and K. Nobe, *J. Electrochem. Soc.* **118** (1971) 545.
16. R. Agrawal and T.K.G. Namboodhiri, *J. Appl. Electrochem.* **22** (1992) 383.
17. N. Elkadar and K. Nobe, *Corrosion* **32** (1976) 128.
18. B. Mernari, H. Elattari, M. Traisnel, F. Bentiss and M. Lagrenee, *Corros. Sci.* **40** (1998) 391.
19. F. Bentiss, M. Lagrenee, M. Traisnel and J.C. Hornez, *Corros. Sci.* **41** (1999) 789.
20. Alan R. Katritzky, S. Rachwal and B. Rachwal, *J. Chem. Soc. Perkin Trans. I* (1987) 799.
21. P. Mathur and T. Vasudevan, *Corrosion* **38** (1982) 17.
22. 'Standard Practice For Laboratory Immersion Corrosion Testing of Metals' (ASTM 1990) 31–72.
23. J.G.N. Thomas, *in* L.L. Shreir, (Ed), 'Corrosion', Vol 2, 2nd edn, Chapter 18, 36. (Newness–Butterworths, London, 1979).
24. N. Hackerman, E.S. Snavely and J.S. Payne, *J. Electrochem. Soc.* **113** (1966) 677.
25. T. Murakawa, S. Nagaura and N. Hackerman, *Corros. Sci.* **7** (1967) 79.
26. F. Mansfeld, *Corrosion* **36** (1981) 301; *Corrosion* **38** (1982) 570.
27. F. Mansfeld, M.W. Kending and S. Tsai, *Corrosion* **37** (1981) 301; *Corrosion* **38** (1982) 570.
28. T. Tsuru, S. Haruyama and B. Gijutsu, *J. Japan Soc. Corros. Engg.* **27** (1978) 573.
29. F. Bentiss, M. Traisnel and M. Largrenee, *Brit. Corros. J.* **35** (2000) 315.
30. E.Mc. Cafferty and N. Hackerman, *J. Electrochem. Soc.* **119** (1972) 146.
31. S. Muralidharan, K.L.N. Phani, S. Pitchumani, S. Ravichandran and S.V.K. Iyer, *J. Electrochem. Soc.* **142** (1995) 1478.